Scalar resonances: Chiral Breit-Wigner expressions

L. O. Arantes* and M. R. Robilotta†

Instituto de Física, Universidade de São Paulo, C.P. 66318, 05315-970, São Paulo, SP, Brazil

Generalized Breit-Wigner expressions describing both single and coupled scalar resonances are derived by combining chiral symmetry and unitarization. Bare scalar propagators are dressed by two-pion loops, results are analytical, and there is little model dependence, since no form factors are used. In the single resonance case, two free coupling parameters are present, which allow flexible descriptions of masses, widths, and pole positions. The usual K-matrix unitarization procedure is recovered as an approximation. When two resonances are present, intermediate pion loops give rise to a coupled channel problem and there is no simple relationship between the unitarized amplitude and Breit-Wigner expressions for individual resonances. Eventually, we approximate and generalize our results and give friendly expressions that can be used in the parametrization of scalar resonances in data analyses.

I. INTRODUCTION

An important feature of quantum chromodynamics (QCD), the basic theoretical framework for hadronic processes, is the prediction of a nontrivial vacuum. At low energies, this vacuum is dominated by quark-antiquark condensates and allows for gentle excitations, such as pions, kaons or etas. These pseudo-Goldstone bosons are highly collective states, which can be neatly perceived by experiment, since their quantum numbers are different from those of the vacuum and a clear contrast is possible.

The situation is much more complex in the case of scalar-isoscalar mesons, which have proved to be the most elusive states in low-energy hadron physics. At present, after decades of research, one still is not sure as how to classify them into multiplets or what their quark and gluon contents are [1]. On the empirical side, one also finds important uncertainties in masses, widths, or even in the very existence of some states.

The interest in the scalar sector was revived recently by evidences provided by the E791 Fermilab experiment of resonances with low masses and large widths in the decays $D^+ \to (\pi^-\pi^+)\pi^+$ [2] and $D_s^+ \to (K^-\pi^+)\pi^+$ [3]. The former finding was confirmed in a number of other reactions: $D^0 \to K_s^0(\pi^-\pi^+)$ [4–6], $\phi \to \gamma(\pi^-\pi^+)$ [7], $J/\psi \to \omega(\pi^-\pi^+)$ [8], and $B^+ \to (\pi^-\pi^+)\pi^+$ [9]. The extraction of information from experiments of this kind is rather involved and normally relies on expressions for resonance widths and amplitudes taken from theory. As a consequence, empirical values for masses and coupling constants depend heavily on the theoretical input used in data analyses. For instance, in Ref. [8], the same data set yields the central values $[M_\sigma, \Gamma_\sigma] = [384, 458]$ MeV, $[442, 346]$ MeV, and $[559, 566]$ MeV, for different theoretical expressions used in the analyses.

At present, the fact is well established that, at low energies, the problems associated with the non-Abelian structure of QCD can be reliably circumvented by means of effective theories. These theories mimic QCD and, in order to be really effective, they must be Poincaré invariant and possess approximate either $SU(2) \times SU(2)$ or $SU(3) \times SU(3)$ symmetries, broken by the small Goldstone boson masses.

The motivation for the present work is to discuss the role of chiral symmetry in the production of scalar resonances at low energies and to derive theoretically sound expressions which may be useful in data analyses. An important dynamical aspect of this problem is that resonances with the same quantum numbers can couple through intermediate states containing two pseudoscalar particles. So, they correspond to the diagonal components of a complex system and the parameters of a light and broad resonance can be strongly influenced by the existence of heavier partners. Therefore we also pay some attention to resonance coupling in the framework of chiral symmetry. For the sake of simplicity, we restrict ourselves to the $SU(2)$ sector.

About ten years ago, Törnqvist [10] discussed both chiral symmetry and resonance couplings in this problem. In his work, the symmetry was enforced by imposing that a background of undisclosed origin should partially cancel pion loop contributions obtained by means of the unitarized quark model, so as to yield the Adler zero of the pion-pion amplitude. The corresponding resonance width for S-wave pions reads

$$\Gamma(s) = \alpha(2s - \mu^2)\frac{\sqrt{s - 4\mu^2}}{\sqrt{s}}e^{-(s-M_r^2)/4\beta^2}, \qquad (1)$$

where α and β are free parameters and μ and M_r are the pion and resonance masses. This prescription is widely used [8,11] and has the merit of including the chiral factor $(2s - \mu^2)$, which makes the width small at low energies. As we discuss in the sequence, effective Lagrangians allow this factor to be reproduced in a natural way and, at the

*Electronic address: lecio@if.usp..br
†Electronic address: robilotta@if.usp.br

same time, give rise to more general expressions, which include other forms of s-dependence. Another advantage of a Lagrangian framework is that it allows the unambiguous separation between resonance and background contributions to the unitarized amplitude. The latter do not include contact terms as in Ref. [10] and are given by just t and u channel singularities [12]. Hence, at the end, there are no large nonresonating backgrounds and the risk of double counting is eliminated.

Our paper is organized as follows. In Sec. II, we review the main features of both linear σ-model and nonlinear chiral descriptions of tree $\pi\pi$ amplitudes. These results allow one to derive a unitarized amplitude for the single resonance case, in Sec. III, which corresponds to a chiral version of the usual Breit-Wigner formula. This is done by resumming a Dyson series in the s-channel and the result is more general than that derived by means of K-matrix unitarization, due to the inclusion of pion off-shell effects. In Sec. IV, we extend the discussion to the case of two resonances and argue that the description of this system by means of two independent Breit-Wigners is very inconvenient. Finally, in Sec. V, we summarize our results and give a simple expression that can be applied in data analyses. We have tried to make this section as self-contained as possible, so that it could be read directly by those people not interested in technical aspects of the calculation. There are also four appendices devoted to technical details.

II. CHIRAL SYMMETRY

The intense activity on chiral perturbation theory performed in the last 20 years has made clear the convenience of working with nonlinear realizations of the symmetry. On the other hand, when dealing with scalar resonances, one may be tempted to employ the old and well-known linear σ-model. The advantage of the former is that it is more general and incorporates all the possible freedom compatible with the symmetry. On the other hand, it is nonrenormalizable and one has to resort to order-by-order renormalization in order to deal with this difficulty. The less general linear model is not affected by this problem.

In order to establish the notation, in this section we review some well-known results for low-energy $\pi\pi$ scattering. Quite generally, the amplitude $T_{\pi\pi}$ for the process $\pi^a(p)\pi^b(q) \rightarrow \pi^c(p')\pi^d(q')$ can be written as [13]

$$T_{\pi\pi} = \delta_{ab}\delta_{cd}A(s, t, u) + \delta_{ac}\delta_{bd}A(t, u, s) + \delta_{ad}\delta_{bc}A(u, s, t), \quad (2)$$

with $s = (p + q)^2$, $t = (p - p')^2$, and $u = (p - q')^2$. A resonance has a well-defined isospin and one uses the decomposition

$$T_{\pi\pi} = T_0(s, t)P_0 + T_1(s, t)P_1 + T_2(s, t)P_2, \quad (3)$$

where P_I is the projection operator into the channel with total isospin I and the amplitudes T_I are given by

$$T_0(s, t) = 3A(s, t, u) + A(t, u, s) + A(u, s, t),$$
$$T_1(s, t) = A(t, u, s) - A(u, s, t), \quad (4)$$
$$T_2(s, t) = A(t, u, s) + A(u, s, t).$$

In the framework of chiral symmetry, the inclusion of resonances must be performed in such a way as to preserve the low-energy theorem for $\pi\pi$ scattering, which ensures that the functions $A(s, t, u)$ must have the form [14]

$$A(s, t, u) = \frac{s - \mu^2}{f_\pi^2} + \cdots, \quad (5)$$

where μ and f_π are the pion mass and decay constant and the ellipsis indicates higher order contributions.

When a scalar-isoscalar resonance is present, the tree-level amplitude for $\pi\pi$ scattering is given by the four diagrams of Fig. 1, irrespective of whether the symmetry is implemented linearly or not. We begin by considering the linear σ-model, described by the Lagrangian

$$\mathcal{L}_\sigma = \frac{1}{2}(\partial_\mu\sigma\partial^\mu\sigma + \partial_\mu\boldsymbol{\pi} \cdot \partial^\mu\boldsymbol{\pi}) - \frac{m^2}{2}(\sigma^2 + \boldsymbol{\pi}^2)$$
$$- \frac{\lambda}{4}(\sigma^2 + \boldsymbol{\pi}^2)^2 + c\sigma. \quad (6)$$

Denoting by s the fluctuations of the scalar field and using $\sigma = f_\pi + s$, one finds, at tree level,

$$\mu^2 = m^2 + \lambda f_\pi^2, \qquad c = \mu^2 f_\pi, \qquad M_\sigma^2 = 2\lambda f_\pi^2 + \mu^2, \quad (7)$$

M_σ being the s mass. The $\pi\pi$ scattering amplitude is

$$A_t(s, t, u) = -2\lambda - \frac{4\lambda^2 f_\pi^2}{s - M_\sigma^2} = \frac{s - \mu^2}{f_\pi^2} - \frac{(s - \mu^2)^2}{f_\pi^2(s - M_\sigma^2)}, \quad (8)$$

where the subscript t stands for *tree*. The contributions on the right-hand side proportional to λ and λ^2 arise, respectively, from the four-pion vertex and one of the resonance terms in Fig. 1 and are not isolately compatible with the low-energy theorem. However, consistency becomes explicit when they are added together, since $M_\sigma^2 \gg \mu^2 \sim s$. This result shows that, in the linear model, the resonance and the nonresonating background must always be treated in the same footing, for the sake of preserving chiral symmetry.

In the alternative approach, the scalar field f couples to pion fields $\boldsymbol{\phi}$, which behave nonlinearly under chiral transformations [15]. This field f is now assumed to be a true chiral scalar, invariant under both vector and axial transformations, and should not be confused with σ, the chiral partner of the pion in the linear σ-model. The effective Lagrangian for this system is written as [16]
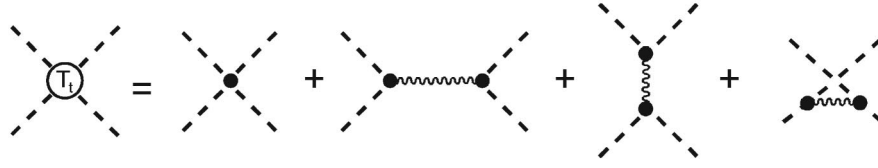
FIG. 1. Tree amplitude T_t; dashed and thin wavy lines represent pions and a scalar resonance.

$$\mathcal{L} = \frac{1}{2}(\partial_\mu f \partial^\mu f - M_\sigma^2 f^2) + \frac{1}{2}\left(1 + c_s \frac{f}{f_\pi}\right)(\partial_\mu \boldsymbol{\phi} \cdot \partial^\mu \boldsymbol{\phi}$$

$$+ \partial_\mu \sqrt{f_\pi^2 - \boldsymbol{\phi}^2} \partial^\mu \sqrt{f_\pi^2 - \boldsymbol{\phi}^2})$$

$$+ \mu^2 f_\pi \left(1 + c_b \frac{f}{f_\pi}\right)(\sqrt{f_\pi^2 - \boldsymbol{\phi}^2} - f_\pi), \quad (9)$$

where the dimensionless constants c_s and c_b represent, respectively, the scalar-pion couplings that preserve and break chiral symmetry.

The evaluation of the diagrams of Fig. 1 then yields

$$A_t(s, t, u) = \frac{s - \mu^2}{f_\pi^2} - \frac{[c_s s/2 - (c_s - c_b)\mu^2]^2}{f_\pi^2(s - M_\sigma^2)}, \quad (10)$$

where, as before, the two terms are due, respectively, to the four-pion vertex and to the resonance. In this case, however, each contribution conforms independently with the low-energy theorem. The former gives rise to the leading term of Eq. (5) and the latter corresponds to a higher order correction. We note that, for $c_s = 2$ and $c_b = 1$, one recovers the result from the linear σ-model, given by Eq. (8). Results from the nonlinear Lagrangian are more general, since they hold for any choices of the parameters c_s and c_b. On the other hand, they are not renormalizable, because the coupling constant c_s/f_π carries a negative dimension. Denoting by $q \sim \mu \sim \sqrt{s}$ the low-energy scale, one learns from Eqs. (8) and (10) that the $\mathcal{O}(q^2)$ leading term is unique whereas the other contributions are $\mathcal{O}(q^4)$ and model dependent. It is important to note that, in order to preserve this chiral hierarchy, the parameters c_s and c_b cannot be too large: they must be smaller than M_σ/μ.

Using results (2), (3), and (10) and projecting into the S-wave channel, we find the following scalar-isoscalar tree-level $\pi\pi$ amplitude [17]:

$$T_t = \frac{2s - \mu^2}{f_\pi^2} - \frac{3[c_s s/2 - (c_s - c_b)\mu^2]^2}{f_\pi^2(s - M_\sigma^2)} + \frac{B(s)}{f_\pi^2}, \quad (11)$$
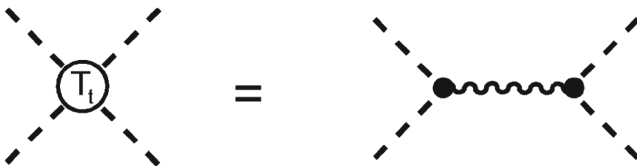
FIG. 2. Tree amplitude T_t; the thick wavy line represents the amplitude T_t, given by Eq. (13).

where the first term implements the low-energy theorem, the second one describes the resonance, and the last function is a nonresonating background, given by

$$B(s) = \left[\frac{c_s^2}{4}(s - 2M_\sigma^2) + c_s(c_s - 2c_b)\mu^2 \right.$$

$$\left. + \frac{2[c_s M_\sigma^2/2 - (c_s - c_b)\mu^2]^2}{s - 4\mu^2} \ln\left(1 + \frac{s - 4\mu^2}{M_\sigma^2}\right)\right].$$

$$(12)$$

This background receives contributions from t and u channels only and, as the resonance term, it is $\mathcal{O}(q^4)$. With future purposes in mind, we rewrite Eq. (11) in a compact form, as

$$T_t = -\frac{\gamma^2}{s - M_\sigma^2}, \quad (13)$$

with

$$\gamma^2(s) = [(2s - \mu^2)(M_\sigma^2 - s) + \eta]/f_\pi^2, \quad (14)$$

$$\eta(s) = 3[c_s s/2 - (c_s - c_b)\mu^2]^2 + B(M_\sigma^2 - s). \quad (15)$$

In evaluating the effects of pion loops, it is useful to associate diagrams directly with Eq. (13). We do this by reexpressing the $\pi\pi$ amplitude of Fig. 1 as in Fig. 2, where the thick wavy line now includes contributions from the four-pion contact interaction, the full s-channel resonance, and t and u exchanges. The function $\gamma(s)$ implements the effective couplings at the vertices.

III. SINGLE RESONANCE AMPLITUDE

Quite generally, the unitarization procedure allows one to extend the range of validity of an amplitude calculated by means of field theory. In the case of the $\pi\pi$ amplitude, it also provides an alternative formulation to the usual chiral perturbation theory [18]. In order to unitarize the $\pi\pi$ amplitude, we consider iterated contributions from a single loop. In this approximation, the dressed propagator is determined by the three diagrams shown in Fig. 3(a). The last of them corresponds to a composite Dyson series and includes all possible iterations of the $\pi\pi$ tree amplitude, as represented in Fig. 3(b). In the sequence we concentrate on the unitarized elastic $\pi\pi$ scattering amplitude and leave a discussion of the dressed resonance propagator to Appendix C.
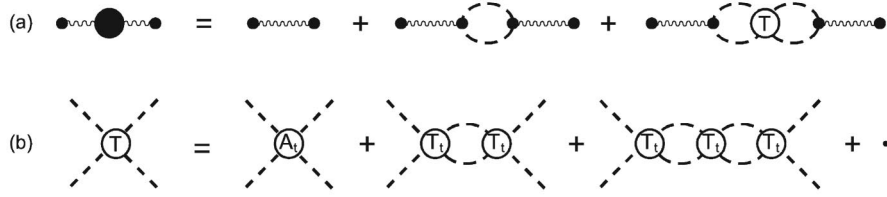
FIG. 3. Full resonance propagator (a) and s-channel unitarized $\pi\pi$ amplitude (b).

The one-loop contribution to the $\pi\pi$ scattering amplitude is given by

$$T_1(s) = T_t[-\Omega]T_t, \qquad (16)$$

where the function

$$\Omega(s) = -\frac{1}{32\pi^2}[L + \Lambda_\infty] \qquad (17)$$

contains an infinite constant Λ_∞ and a finite component $L(s)$, which can be evaluated analytically and is given in Appendix A.

In the linear σ-model, singularities introduced by loops can be removed consistently. The renormalization of the σ-model was discussed by Lee and collaborators [17,19], reviewed in a pedagogical way in Ref. [20], and adapted to this problem in Appendix B. This procedure entitles one to replace Λ_∞ in Eq. (16) by a yet undetermined constant c. Denoting by $\bar{\Omega}$ this new function and by $\bar{R}$ and I its real and imaginary parts, the usual self-energy insertion is written as

$$\bar{\Sigma}(s) = \gamma^2[\bar{R} + iI]. \qquad (18)$$

Considering all possible iterations of the two-pion loop, we construct the full s-channel $\pi\pi$ amplitude given in Fig. 3(b). This geometrical series can be summed and one finds

$$\bar{T}(s) = \frac{T_t}{1 + \bar{\Omega}T_t}. \qquad (19)$$

This result can be reexpressed by defining a running mass $\mathcal{M}$ and a width Γ such that

$$\bar{T}(s) = -\frac{\gamma^2}{s - \mathcal{M}^2 + iM_\sigma\Gamma}, \qquad (20)$$

with $\mathcal{M}^2(s) = M_\sigma^2 + \gamma^2\bar{R}$ and $M_\sigma\Gamma(s) = \gamma^2 I$. We fix the constant c by imposing that the pole of $\bar{T}$ occurs at the physical mass M_σ, which corresponds to the condition $\bar{R}(M_\sigma^2) = 0 \rightarrow c = -\Re L(M_\sigma^2)$. The running mass and width become

$$\mathcal{M}^2(s) = M_\sigma^2 + [(2s - \mu^2)(M_\sigma^2 - s) + \eta]$$
$$\times [\bar{R}(s) - \bar{R}(M_\sigma^2)]/f_\pi^2, \qquad (21)$$

$$\Gamma(s) = [(2s - \mu^2)(M_\sigma^2 - s) + \eta]$$
$$\times \frac{\sqrt{s - 4\mu^2}}{32\pi f_\pi^2 M_\sigma\sqrt{s}}\Theta(s - 4\mu^2), \qquad (22)$$

with $\eta(s)$ given by Eq. (15). The signature of chiral symmetry in this problem is the factor $(2s - \mu^2)/f_\pi^2$ within square brackets, which implements the low-energy theorem and is due to the use of Eq. (11) as the main building block in the calculation. This is the only $\mathcal{O}(q^2)$ term and it dominates at low energies. On the other hand, as s approaches M_σ^2, the relative importance of the various contributions changes and the model dependent factor proportional to η dominates. These results correspond to the most general expression possible for the running mass and width dictated by chiral symmetry. The latter is to be compared with Eq. (1). The presence of the parameters c_s and c_b allows for a wide variety of forms for the width. In particular, when $c_s = 0$, one can expect a resonance with a rather low intensity. As far as the background is concerned, its importance cannot be large at low energies, since it is $\mathcal{O}(q^4)$ and does not contribute at the resonance pole.

In Fig. 4, we explore the interplay between chiral symmetry and resonance in the function $|T(s)|^2$. For the sake of using a round number, the scalar mass was fixed at $M_\sigma = \sqrt{12}\mu \sim 485$ MeV. The first term of Eq. (11) yields the *leading order* curve, an unbound parabola which blows up at large energies. The inclusion of the remaining two terms in that amplitude gives rise to the *tree* curve. The *unitarized σ-model* curve, given by Eq. (20) with ($c_s = 2$, $c_b = 1$), is
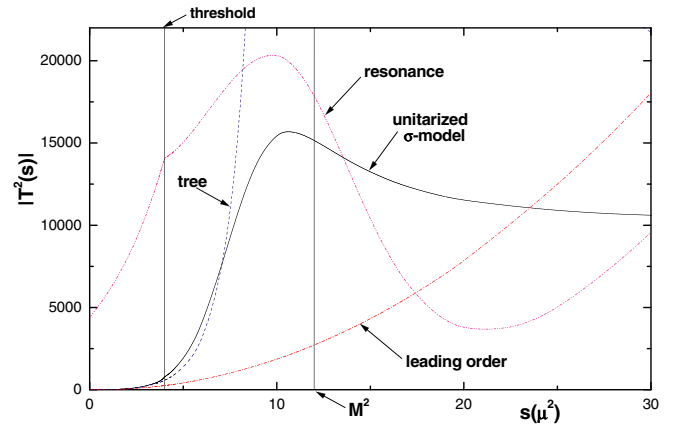

FIG. 4 (color online). The functions $T(s)$ are $\pi\pi$ amplitudes; the first term of Eq. (11) corresponds to the *leading order* (dash-dotted) curve, the full equation is represented by the *tree* (dashed) curve, Eq. (20) with ($c_s = 2$, $c_b = 1$) gives rise to the *unitarized σ-model* (continuous) curve and the *resonance* (dotted) curve is derived by iterating just the term proportional to λ^2 in Eq. (8) and then adding that proportional to λ.

obtained by iterating the *tree* amplitude by means of two-pion loops. Finally, the *resonance* curve is derived by iterating just the term proportional to λ^2 in Eq. (8) and then adding that proportional to λ. Inspecting this figure, one learns that the proper implementation of chiral symmetry in this problem ensures that the *leading order*, *tree* and *unitarized σ-model* curves stay very close together at low energies. We have exemplified this kind of behavior in the case of the σ-model, but it holds for other choices of the parameters (c_s, c_b) as well. As far as the *resonance* curve is concerned, chiral symmetry is badly violated, since it does not tend to the *leading order* one when $s \rightarrow 0$, as predicted by the low-energy theorem. The reason for this kind of deviation can be traced to the fact that loop contributions become rather large when one iterates just the term proportional to λ^2 in Eq. (8).

The free parameters (c_s, c_b) in Eqs. (21) and (22) allow a rather flexible relationship between mass and width, which is exemplified in Tables I, II, and III. Predictions for the choice $(c_s = 2, c_b = 1)$, corresponding to the σ-model, are given in Table I. In Table II, we show that empirical values quoted in the literature can be easily encompassed by suitable choices of the free parameters. Finally, Table III is related to the recent analysis of elastic $\pi\pi$ scattering in the framework of chiral perturbation theory, produced by Colangelo, Gasser, and Leutwyler [21]. In their work, one finds a precise expression for the isoscalar S-wave phase shift, valid for energies below 1 GeV and given by[1]

$$\tan\delta_0^0 = \frac{\sqrt{s - 4\mu^2}}{\sqrt{s}}[a + bs/\mu^2 + cs^2/\mu^4 + ds^3/\mu^6]$$
$$\times \frac{4\mu^2 - s_0}{s - s_0}, \tag{23}$$

where $a = -6.051 \times 10^{-2}$, $b = 7.291 \times 10^{-2}$, $c = -6.08 \times 10^{-4}$, $d = -2.2 \times 10^{-5}$, and $s_0 = (846 \text{ MeV})^2$. The corresponding scattering amplitude is given by Eq. (20), with $\gamma^2 = 32\pi(s_o - 4\mu^2)[a + bs/\mu^2 + cs^2/\mu^4 + ds^3/\mu^6]$ and $\Gamma(s) = \gamma^2\sqrt{s - 4\mu^2}/32\pi M_\sigma\sqrt{s}$. The resonance parameters are $M_\sigma = 846$ MeV and $\Gamma(M_\sigma) = 532$ MeV, whereas the denominator of the scattering amplitude vanishes at $\sqrt{s} = (454.73 - i290.25)$ MeV. In this channel, as pointed out in Ref. [21], physical parameters are very different from the pole position due to the strong s dependence in the numerator of Eq. (23), manifest in the fact that the parameters a and b are comparable.[2] This important feature is inherent to the isoscalar channel, since the resonance, which is a nonleading chiral effect, must always coexist with a strong

---

[1]This is Eq. (17.2) of Ref. [21], translated into our notation.
[2]As an exercise, we eliminated the strong s dependence by making $b = c = d = 0$ in Eq. (23), adopted the value $a = 0.220$ prescribed in Ref. [21] and found the physical parameters $M_\sigma = 846.00$ MeV, $\Gamma(M_\sigma) = 156.65$ MeV, and the pole position at $\sqrt{s} = (849.08 - i78.23)$ MeV.

TABLE I.   Relation between masses and widths in the linear σ-model.

M_σ (MeV)	350	400	450	500	550	600	650	700	750	800	850
Γ (MeV)		63	121	201	304	432	589	778	1000	1258	1555	1894

TABLE II.   Some empirical masses and widths reproduced by choices of coupling parameters.

Reference	M_σ (MeV)	Γ_σ (MeV)	c_s	c_b
[8]	384	458	4.68	1
[8]	442	346	2.81	1
[2]	478	324	2.28	1
[8]	559	566	2.24	1

TABLE III.   Some masses, widths, and coupling parameters which reproduce the pole at $\sqrt{s} = (454.73 - i290.25)$ MeV [21].

M_σ (MeV)	Γ_σ (MeV)	c_s	c_b
331.76	365.93	0.590	12
403.77	333.58	0.594	10
688.22	757.10	1.150	8

polynomial variation in s, required by the low-energy chiral behavior. A discussion of this problem in the framework of the linear σ-model can be found in Ref. [22]. In Table III, we show a sample of parameters that reproduce the $\sqrt{s}$ pole quoted above [21].

In Fig. 5 we compare the behavior of the widths as given by Eqs. (1) and (22). The parameter α of the former was tuned so that $\Gamma(M_\sigma)$ is the same in both cases, whereas $\beta = 700$ MeV [11]. We also include a curve representing
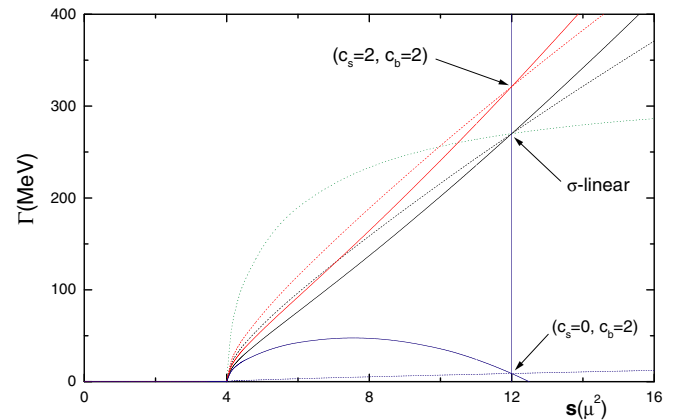

FIG. 5 (color online).   Behavior of the resonance width. The full and dashed curves were, respectively, obtained from Eqs. (1) and (22), for the choices of parameters indicated explicitly, whereas the dotted curve corresponds to Eq. (24).

the function

$$\Gamma(s) = \frac{3(M_\sigma^2 - \mu^2)^2}{32\pi f_\pi^2} \frac{\sqrt{s - 4\mu^2}}{M_\sigma \sqrt{s}} \Theta(s - 4\mu^2), \qquad (24)$$

which is obtained by unitarizing just the term proportional to λ^2 in Eq. (8), a procedure which is not compatible with chiral symmetry. The scalar mass was fixed at $M_\sigma = \sqrt{12}\mu$ and three choices were used for the parameters (c_s, c_b), which control the value of $\Gamma(M_\sigma)$. Results are sensitive to the free parameters in Eq. (22) and, although both forms of the width are compatible with chiral symmetry, differences at low energies may be large.

A straightforward alternative for unitarizing amplitudes is based on the so-called K-matrix formalism [23]. In the scalar-isoscalar channel, the nonrelativistic kernel K is related to the relativistic tree amplitude by

$$K(s) = \frac{T_t}{16\pi\sqrt{s}} \qquad (25)$$

and its on-shell iteration yields the scattering amplitude

$$f = K/(1 - iqK), \qquad (26)$$

where $q = \sqrt{s/4 - \mu^2}$ is the center of mass momentum. Using $qK = \tan\delta$, one finds the usual phase shift parametrization for f. The relativistic counterpart of (26) has the form of Eq. (20) with $\mathcal{M} \to M_\sigma$. This is expected since, as it is well known, K-matrix unitarization gives rise to a width, but does not renormalize the mass. In Fig. 6, we compare the functions $|\bar{T}(s)|^2$ unitarized by either two-pion intermediate states or the K-matrix, for a choice of the parameters (c_s, c_b). The figure shows that the great flexibility of the nonlinear model, which has two free parameters, allows for a wide variation in the form of the amplitude without destroying the compatibility with chiral symmetry. We also note that the K-matrix unitarization does give rise to reasonable approximations, at a rather low
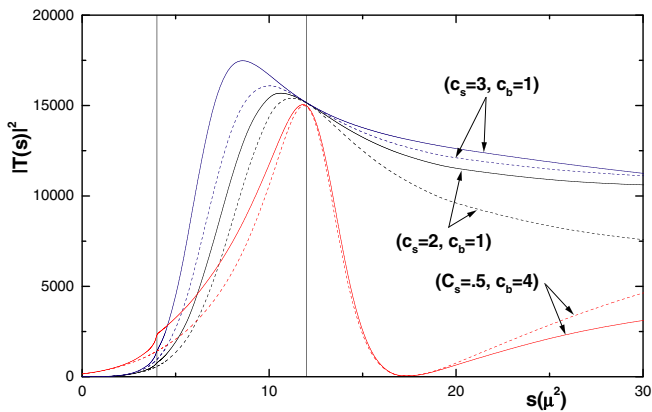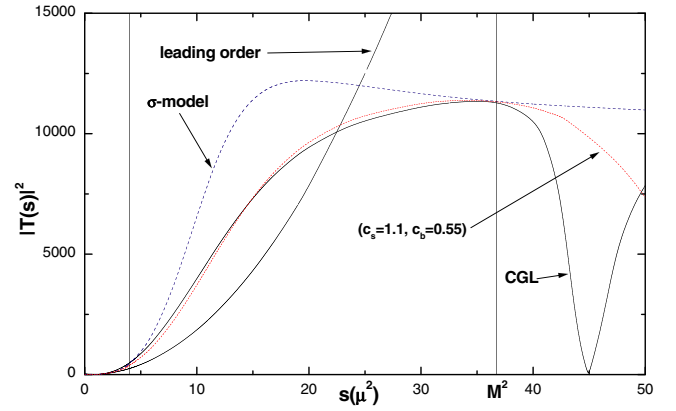

FIG. 7 (color online). The functions $T(s)$ are $\pi\pi$ amplitudes; the continuous, dashed, and dotted curves describe, respectively, the empirical fit from Ref. [21], the linear σ-model prediction, and a crude fit corresponding to the nonlinear parameters ($c_s = 1.10, c_b = 0.55$).

algebraic cost. On the other hand, the comparison between full and dashed curves indicates that loop corrections to the resonance mass may be important at low energies.

In Fig. 7 we display the behavior of the function $|\bar{T}(s)|^2$ for the parameters given in Eq. (23), which summarize experimental results [21] and yield $M_\sigma = 846$ MeV, together with the corresponding prediction from the linear σ-model, unitarized by two loop intermediate states. One notes that the linear model overestimates results in the region $s < M_\sigma^2$, whereas a crude visual fit can be obtained using ($c_s = 1.10, c_b = 0.55$) in the nonlinear interaction. This suggests that data tends to favor the latter.

IV. TWO-RESONANCE AMPLITUDE

The linear σ-model can be generalized so as to encompass two resonances. The extension to the three flavor case has been reviewed in Ref. [24] and applied to the study of scalar mesons in Ref. [23]. As we show in Appendix D, this generalization can also be performed by introducing a second scalar-isoscalar field ξ, which is assumed to be a chiral scalar, without further commitments concerning its physical nature. This allows it to be compatible with any kind of structures outside the SU(2) sector such as, for instance, $s\bar{s}$ or glueball states.

The tree amplitude for $\pi\pi$ scattering for two resonances α and β is represented by the diagrams of Fig. 8 and given by Eq. (D9) of Appendix D. It reads

$$A_t(s, t, u) = \frac{s - \mu^2}{f_\pi^2} - \cos^2\theta \frac{(s - \mu^2)^2}{f_\pi^2(s - M_\alpha^2)}$$
$$- \sin^2\theta \frac{(s - \mu^2)^2}{f_\pi^2(s - M_\beta^2)}, \qquad (27)$$

where θ is a mixing angle, which can be treated as a free parameter. This result corresponds to a generalization of Eq. (8) and is consistent, as it must be, with the low-energy
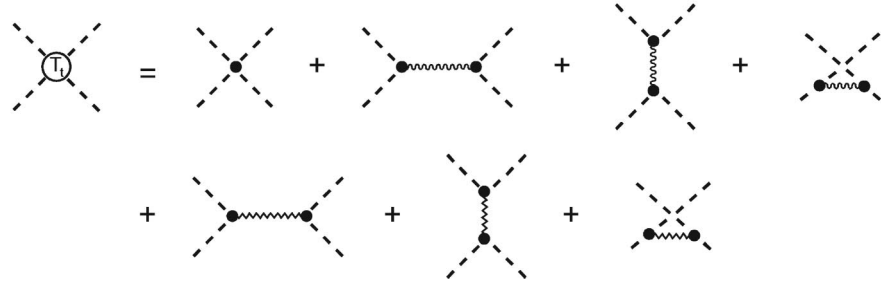

FIG. 6 (color online). Amplitudes unitarized by means of two-pion loops (continuous lines) and K-matrix (dashed lines) for the choices of parameters (c_s, c_b) indicated explicitly.

FIG. 8.   Tree amplitude for coupled resonances; dashed, wavy, and zigzag lines represent pions, and resonances α and β, respectively.

theorem. The implications of Eq. (27) can be understood by noting that, in the large M_β limit, the comparison of Eqs. (10) and (27) motivates a class of departures represented by parameters of the form $c_s = 2c_b = 2\cos\theta$, which is exemplified in Fig. 9. It is interesting to note that, in this case, the coupling with a heavier partner works towards the reduction of the $\pi\pi$ width of particle α by a factor proportional to $\cos\theta^2$. Therefore such a coupling is not instrumental in explaining the nature of a possible broad low-energy resonance.

As in the single resonance case, it is convenient to explore the greater freedom of the nonlinear model. One possibility is to assume that the $\pi\pi$ amplitudes calculated by means of chiral perturbation theory already contain the mechanisms that give rise to the resonance pole [25]. In the framework of quantum field theory, it is more convenient to treat the resonances as explicit degrees of freedom and write the amplitude as

$$A_t(s, t, u) \equiv A_{t\alpha}(s, t, u) + A_{t\beta}(s, t, u)$$
$$= \frac{s - \mu^2}{f_\pi^2} - \frac{[c_s^\alpha(s/2 - \mu^2) + c_b^\alpha \mu^2]^2}{f_\pi^2(s - M_\alpha^2)}$$
$$- \frac{[c_s^\beta(s/2 - \mu^2) + c_b^\beta \mu^2]^2}{f_\pi^2(s - M_\beta^2)}. \tag{28}$$
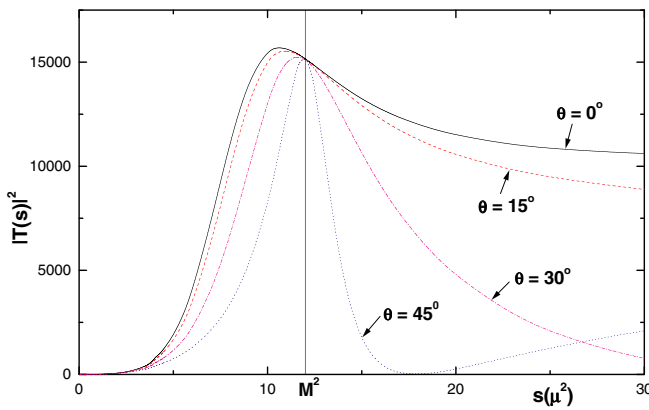

FIG. 9 (color online).   Low-energy behavior of $|T(s)|^2$ in the generalized linear σ-model, for a resonance of mass 485 MeV coupled to a heavier one, as a function of the mixing angle.

This yields a tree scalar-isoscalar amplitude of the form

$$T_t = T_{t\alpha} + T_{t\beta} = -\frac{\gamma_\alpha^2}{s - M_\alpha^2} - \frac{\gamma_\beta^2}{s - M_\beta^2}, \tag{29}$$

where

$$\gamma_i^2(s) = [(2s - \mu^2)(M_i^2 - s)/2 + \eta_i]/f_\pi^2, \tag{30}$$

and the model dependent functions $\eta_i(s)$ are obtained by using the parameters specific to each resonance in Eq. (15). The functions γ_i^2 play the role of effective couplings and, in the evaluation of the unitarized amplitude, it is useful to express T_t as in Fig. 10, where and thick wavy and zigzag lines represent $T_{t\alpha}$ and $T_{t\beta}$, respectively.

In the case of two scalar resonances α and β, which can couple through a two-pion intermediate state, one has to consider the four two-point functions displayed in Fig. 11(a). The structures of these functions are indicated in Fig. 11(b) and depend on the full elastic $\pi\pi$ amplitude.

As in the single resonance case, the $\pi\pi$ amplitude is obtained by iterating T_t. The single loop term reads

$$T_\ell(s) = [T_{t\alpha} + T_{t\beta}][-\Omega][T_{t\alpha} + T_{t\beta}], \tag{31}$$

where Ω is given by Eq. (17) and contains a divergence that needs to be removed by renormalization. In the linear σ-model, the same formal manipulations used in Appendix B allow counterterms to be generated in the two-resonance Lagrangian, and the regularized version of T_ℓ reads

$$\bar{T}_\ell(s) = \sum_{i=\alpha}^{\beta} \sum_{j=\alpha}^{\beta} T_{ti}[-\bar\Omega_{ij}]T_{tj}, \tag{32}$$

FIG. 10.   Tree amplitude T_t; thick wavy and zigzag lines represent the full contribution of scalar resonances α and β to the $\pi\pi$ amplitude.
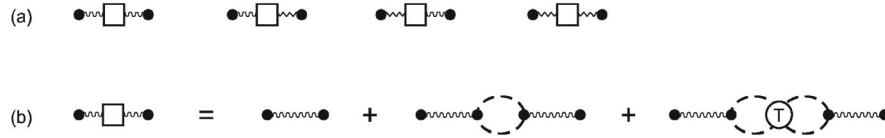
FIG. 11. Coupled resonance propagators (a) and their dynamical structures (b); dashed, wavy, and zigzag lines represent pions and scalar resonances α and β, respectively.

with

$$\bar{\Omega}_{ij}(s) = -\frac{1}{32\pi^2}[L + c_{ij}].\qquad(33)$$

We denote by $\bar{R}_{ij}$ and I the real and imaginary parts of $\bar{\Omega}_{ij}$ and assume that the same kind of counterterms can be used for a minimal regularization in the nonlinear case.

The iteration of this amplitude to all orders gives rise to the structure shown in Fig. 12(a), which contains four subamplitudes, denoted by $\bar{T}_{ij}$. In order to construct these functions, we first evaluate the sum of all two-pion loops involving a single resonance, represented by the black blobs, and recover the result given in Eq. (20). We then assemble all possible combinations of these results, as in Figs. 12(b) and 12(c), and find the diagonal and off-diagonal amplitudes, given by

$$\bar{T}_{\alpha\alpha}(s) = \frac{-\gamma_\alpha^2[s - M_\beta^2 - \gamma_\beta^2(\bar{R}_{\beta\beta} + iI)]}{D + iGI},\qquad(34)$$

$$\bar{T}_{\alpha\beta}(s) = \frac{-\gamma_\alpha^2\gamma_\beta^2(\bar{R}_{\alpha\beta} + iI)}{D + iGI},\qquad(35)$$

with

$$D(s) = (s - M_\alpha^2 - \gamma_\alpha^2\bar{R}_{\alpha\alpha})(s - M_\beta^2 - \gamma_\beta^2\bar{R}_{\beta\beta})$$
$$- \gamma_\alpha^2\gamma_\beta^2(\bar{R}_{\alpha\beta})^2,\qquad(36)$$

$$G(s) = -\gamma_\alpha^2(s - M_\beta^2) - \gamma_\beta^2(s - M_\alpha^2)$$
$$+ \gamma_\alpha^2\gamma_b^2(\bar{R}_{\alpha\alpha} + \bar{R}_{\beta\beta} - 2\bar{R}_{\alpha\beta}).\qquad(37)$$

The expression for $\bar{T}_{\beta\beta}$ is obtained by making $(\alpha \leftrightarrow \beta)$ in Eq. (34). The evaluation of the full s-channel $\pi\pi$ amplitude, Fig. 12(a), produces

$$\bar{T}(s) = \frac{G}{D + iGI}.\qquad(38)$$

In order to determine the counterterms c_{ij} in Eq. (33), one needs three conditions. One of them is obtained by imposing that the resonances decouple at their poles and corresponds to $(\bar{R}_{\alpha\alpha} + \bar{R}_{\beta\beta} - 2\bar{R}_{\alpha\beta}) = 0$. The function $G(s)$ then becomes proportional to the tree amplitude and the unitarized amplitude can be written as

$$\bar{T}(s) = \frac{T_t(s)}{[D/(s - M_\alpha^2)(s - M_\beta^2)] + iT_t(s)I}.\qquad(39)$$

This shows that the zeroes of $\bar{T}(s)$ and $T_t(s)$ coincide, enforcing the idea that "a zero in the partial wave ampli-
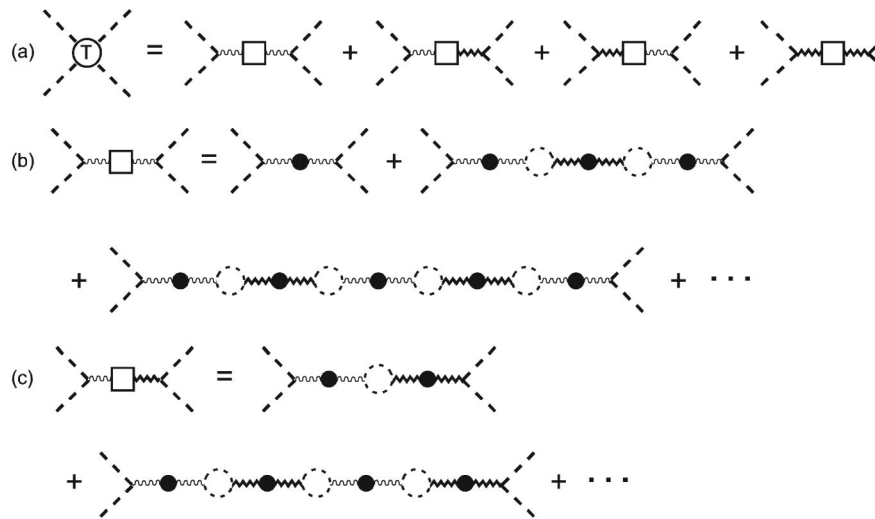

FIG. 12. Coupled resonance contribution to the $\pi\pi$ amplitude (a), which contains diagonal (b) and off-diagonal terms (c). The meaning of the thick wavy and zigzag lines is given in Fig. 10 and the large black blobs indicate the sum of all pion loop diagrams involving a single resonance.

tude in the physical region remains a zero after unitarization," put forward by Törnqvist [10]. The other two conditions are obtained by making $D(M_\alpha^2) = D(M_\beta^2) = 0$ and yield

$$c_{\alpha\alpha} = -[\gamma_\alpha^2(M_\beta^2)\Re L(M_\alpha^2) + \gamma_\beta^2(M_\alpha^2)\Re L(M_\beta^2) - \gamma_\beta^2(M_\alpha^2)(c_{\alpha\alpha} - c_{\beta\beta})]/[\gamma_\alpha^2(M_\beta^2) + \gamma_\beta^2(M_\alpha^2)],$$

$$c_{\beta\beta} = -[\gamma_\alpha^2(M_\beta^2)\Re L(M_\alpha^2) + \gamma_\beta^2(M_\alpha^2)\Re L(M_\beta^2) + \gamma_\alpha^2(M_\beta^2)(c_{\alpha\alpha} - c_{\beta\beta})]/[\gamma_\alpha^2(M_\beta^2) + \gamma_\beta^2(M_\alpha^2)],$$

$$c_{\alpha\alpha} - c_{\beta\beta} = \frac{64\pi^2(M_\beta^2 - M_\alpha^2)}{\gamma_\alpha^2(M_\beta^2) + \gamma_\beta^2(M_\alpha^2)} \left\{ \sqrt{1 + \frac{[\gamma_\alpha^2(M_\beta^2) + \gamma_\beta^2(M_\alpha^2)]\Re[L(M_\beta^2) - L(M_\alpha^2)]}{16\pi^2(M_\beta^2 - M_\alpha^2)}} - 1 \right\}.$$

$$(40)$$

These results determine completely Eq. (38). Its meaning becomes more transparent when it is rewritten as

$$\bar{T}(s) = -\frac{\gamma_\alpha^2(s - M_\beta^2) + \gamma_\beta^2(s - M_\alpha^2)}{(s - \mathcal{M}_\alpha^2)(s - \mathcal{M}_\beta^2) + i[(s - M_\beta^2)M_\alpha\Gamma_\alpha + (s - M_\alpha^2)M_\beta\Gamma_\beta]}, \tag{41}$$

where the running masses are given by

$$\mathcal{M}_{\alpha,\beta}^2(s) = \tfrac{1}{2}\{M_\alpha^2 + \gamma_\alpha^2\bar{R}_{\alpha\alpha} + M_\beta^2 + \gamma_\beta^2\bar{R}_{\beta\beta} \mp \sqrt{(M_\alpha^2 + \gamma_\alpha^2\bar{R}_{\alpha\alpha} - M_\beta^2 - \gamma_\beta^2\bar{R}_{\beta\beta})^2 + \gamma_\alpha^2\gamma_\beta^2(\bar{R}_{\alpha\alpha} + \bar{R}_{\beta\beta})^2}\} \tag{42}$$

and the functions $\Gamma_{\alpha,\beta}(s)$ are obtained by using the parameters suited to each resonance in Eq. (22).

This result is the two-resonance version of Eq. (20). It was obtained by means of standard techniques from quantum field theory, which prescribe that one should first combine the tree-level contributions from the two resonances, as in Eq. (29) and then evaluate loop corrections. A consequence of loop dynamics is that the resonances become interwoven, as it happens in typical coupled channel problems. This feature is especially prominent in the results for the running masses, but still persists when one works in the K-matrix approximation, which corresponds to the replacement $\mathcal{M}_{\alpha,\beta}(s) \to M_{\alpha,\beta}$. In particular, there is no simple relationship between Eq. (41) and Breit-Wigner expressions for individual resonances.

On the other hand, the assumption that resonances behave independently is usual in analyses of empirical data [2,3] and is implemented by means of adjustable complex coefficients. In order to see the problem with such a procedure, let us consider the equation

$$\bar{T}(s) = -\frac{C_\alpha e^{i\delta_\alpha}\gamma_\alpha^2}{(s - M_\alpha^2) + iM_\alpha\Gamma_\alpha} - \frac{C_\beta e^{i\delta_\beta}\gamma_\beta^2}{(s - M_\beta^2) + iM_\beta\Gamma_\beta} = -\frac{\gamma_\alpha^2(s - M_\beta^2) + \gamma_\beta^2(s - M_\alpha^2)}{(s - M_\alpha^2)(s - M_\beta^2) + i[(s - M_\beta^2)M_\alpha\Gamma_\alpha + (s - M_\alpha^2)M_\beta\Gamma_\beta]}, \tag{43}$$

which realizes this idea in the K-matrix approximation. By imposing it to be valid, the free parameters $C_{\alpha,\beta}$ and $\delta_{\alpha,\beta}$ can be easily determined. However, these solutions will depend strongly on the variable s, and it will be extremely difficult to determine their form directly from empirical data. This makes the procedure of adding individual Breit-Wigner structures for resonances with the same quantum numbers to be rather inconvenient in data analyses. The same can be said of treatments based on phase shifts and nonrelativistic quantum mechanics [26].

V. SUMMARY

In this work we have shown how chiral symmetry and unitarization can be combined in order to produce generalizations of the usual Breit-Wigner expression for describing both single and coupled scalar resonances. The motivation for deriving or results was the feeling that the wealth of data on scalar resonances produced by several experimental facilities around the world are not being adequately interpreted in the low-energy region.

Chiral symmetry.—At present, the most reliable theoretical methods for implementing QCD at low energies rely on chiral symmetry. This symmetry is especially suited for describing processes involving pions and has been successfully applied to a rather large sample of physical problems [27]. Resonances manifest themselves as poles in the second Riemann sheet of scattering amplitudes and chiral symmetry is essential in explaining [21] how the scalar parameters $(M_\sigma, \Gamma_\sigma/2) \simeq (846, 265)$ MeV can be compatible with a pole position at $\sqrt{s} \simeq (455 - i290)$ MeV. In the case of scalar resonances, which couple strongly to pions, a failure to incorporate chiral symmetry into data analyses cannot be theoretically justified.

Unitarization.—In the framework of quantum field theory, the pole structure associated with a resonance can be generated by assuming that it has a definite mass in the Lagrangian and then turning on the interaction that allows

it to decay. In the case of a scalar resonance, this gives rise to a dressed propagator constructed by summing all the iterations of the bare propagator and two-pion loops. The advantage of this procedure is that there is little model dependence: one does not use form factors and the loop contribution is given by a compact analytical expression, which is real below threshold and complex afterwards. This kind of dynamical unitarization gives rise both to a width and a running mass.

Single resonance.—In Sec. III we have constructed a chiral Breit-Wigner suited for a single scalar resonance [Eqs. (20)–(22)], with the following properties:

   (i) at low energies, it reproduces (Fig. 4) the theorem derived by Weinberg [14] for $\pi\pi$ scattering;

  (ii) it is compatible with a rather general nonlinear realization of chiral symmetry, which involves two free parameters, and incorporates the linear σ-model as a particular case;

 (iii) the only constraint on these parameters is that they must be smaller than M_σ/μ;

 (iv) the presence of two free parameters allows a rather flexible description of masses, widths, and pole positions;

  (v) results form the usual K-matrix unitarization can be recovered as reasonable approximation (Fig. 6), when the running mass is replaced by that of the resonance.

We are aware that complicated expressions are not useful in data analyses. Therefore we simplify our results from Sec. III and propose the following chiral Breit-Wigner expression as a trial function:

$$\bar{T}(s) = -\frac{\gamma^2}{s - M^2 + iM\Gamma}, \qquad (44)$$

with

$$\Gamma(s) = \gamma^2 \frac{\sqrt{s - 4\mu^2}}{32\pi M\sqrt{s}}\Theta(s - 4\mu^2). \qquad (45)$$

$$\gamma(s) = \{(2s - \mu^2)(M^2 - s)$$
$$+ 3[c_s s/2 - (c_s - c_b)\mu^2]^2\}/f_\pi^2. \qquad (46)$$

It incorporates the essential features of chiral symmetry and M, c_s, and c_b can be treated as adjustable parameters. This function generalizes that produced by Törnqvist [10] about ten years ago, which corresponds to using $\gamma^2(s) = \alpha(2s - \mu^2)$, where α is a free constant.

Two resonances.—The coupling of two resonances with the same quantum numbers was discussed in Sec. IV and we have restated within a Lagrangian framework several results derived in Ref. [10], namely, that:

   (i) both the σ-linear and nonlinear chiral models can be extended in order to include more than one resonance;

  (ii) dynamical unitarization by means of quantum field theory techniques corresponds to first combining tree-level resonance amplitudes and subsequently evaluating loop corrections;

 (iii) this procedure ensures that a zero in the tree amplitude remains a zero after unitarization;

 (iv) in the coupled channel problem, there is no simple relationship between the unitarized amplitude and Breit-Wigner expressions for individual resonances;

  (v) the price to be paid for representing each resonance by a Breit-Wigner is a very high one, since one will have to deal with coefficients and phases that depend strongly on the variable s.

In the two-resonance case, the following trial function can be used:

$$\bar{T}(s) =$$
$$-\frac{\gamma_\alpha^2(s - M_\beta^2) + \gamma_\beta^2(s - M_\alpha^2)}{(s - M_\alpha^2)(s - M_\beta^2) + i[(s - M_\beta^2)M_\alpha\Gamma_\alpha + (s - M_\alpha^2)M_\beta\Gamma_\beta]}, \qquad (47)$$

where $\Gamma_{\alpha,\beta}$ and $\gamma_{\alpha,\beta}$ are obtained by using the parameters suited for each resonance in Eqs. (45) and (46).

ACKNOWLEDGMENTS

APPENDIX A: LOOP INTEGRAL

The function $L(s)$, which determines the self-energy associated with a s-channel loop, Eq. (17), is given by

$$0 \le s < 4\mu^2 \to L(s) = -2\frac{\sqrt{4\mu^2 - s}}{\sqrt{s}}\tan^{-1}\left[\frac{\sqrt{s}}{\sqrt{4\mu^2 - s}}\right], \qquad (A1)$$

$$4\mu^2 \le s \to L(s)$$
$$= \frac{\sqrt{s - 4\mu^2}}{\sqrt{s}}\left\{\ln\left[\frac{\sqrt{s} - \sqrt{s - 4\mu^2}}{\sqrt{s} + \sqrt{s - 4\mu^2}}\right] + i\pi\right\}. \qquad (A2)$$

Its behavior is displayed in Fig. 13, where it is possible to notice a cusp at $s = 4\mu^2$. As discussed in Sec. III, the renormalization procedure introduces a constant c into Eq. (17), which becomes

$$\bar{\Omega}(s) = -\frac{1}{32\pi^2}[L + c]. \qquad (A3)$$

As a consequence, the form of the function $\bar{R}(s)$, describing off-shell effects in pion loops, can be inferred
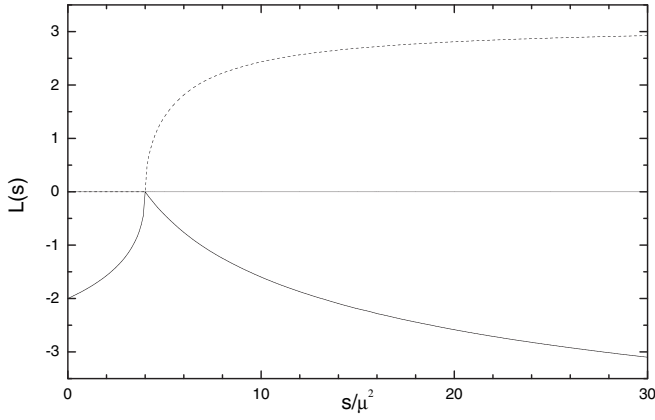
FIG. 13. Function $L(s)$, which determines the self-energy associated with the loop.

directly from Fig. 13, by shifting vertically its real part by c.

APPENDIX B: RENORMALIZATION

In order to keep only the essential features of the problem, one notes that the dynamical scalar mass can be cut along a $\pi\pi$ loop, whereas the pion mass can be cut along a $\pi\sigma$ loop. As the latter is heavier, we assume that changes in the pion mass can be neglected at the energy scale one is working at. The lifting of this restriction is straightforward, but would require a considerable increase in the algebraic effort. Since at one-loop level the wave function renormalization is finite [20], the elimination of Λ_∞ from Eq. (17) is performed by making $m \to m_0$ and $\lambda \to \lambda_0$ in Eq. (6) and rewriting it as

$$
\begin{aligned}
\mathcal{L}_\sigma = \frac{1}{2}(\partial_\mu \sigma \partial^\mu \sigma + \partial_\mu \boldsymbol{\pi} \cdot \partial^\mu \boldsymbol{\pi}) - \frac{m^2}{2}(\sigma^2 + \boldsymbol{\pi}^2) \\
- \frac{\lambda}{4}(\sigma^2 + \boldsymbol{\pi}^2)^2 + f_\pi \mu^2 \sigma - \frac{\delta_m}{2}(\sigma^2 + \boldsymbol{\pi}^2) \\
- \frac{\delta_\lambda}{4}(\sigma^2 + \boldsymbol{\pi}^2)^2,
\end{aligned}
\tag{B1}
$$

with $\delta_m = m_0^2 - m^2$ and $\delta_\lambda = \lambda_0 - \lambda$. Expanding σ around f_π, using the condition $\delta_m = -f_\pi^2 \delta_\lambda$ associated with the constancy of μ^2 and noting that tadpoles do not contribute by construction [20], one finds

$$
\begin{aligned}
\mathcal{L} = \frac{1}{2}(\partial_\mu f \partial^\mu f - M_\sigma^2 f^2) + \frac{1}{2}(\partial_\mu \boldsymbol{\pi} \cdot \partial^\mu \boldsymbol{\pi} - \mu^2 \boldsymbol{\pi}^2) \\
- \lambda f_\pi f \boldsymbol{\pi}^2 - \lambda \boldsymbol{\pi}^4 + \cdots - \delta_\lambda (f_\pi^2 f^2 + f_\pi f \boldsymbol{\pi}^2 \\
+ \boldsymbol{\pi}^4/4 + \cdots).
\end{aligned}
\tag{B2}
$$

This result gives rise to the counterterm diagrams shown in Fig. 14, which allow the factor Λ_∞ in Eq. (17) to be killed by a suitable choice of δ_λ. We are then entitled to replace Λ_∞ in Eq. (17) by a finite constant c.

APPENDIX C: SCALAR PROPAGATOR

The full scalar propagator is given in Fig. 3 and can be evaluated using the results of Sec. III. It reads

$$
\bar{\Delta}(s) = \frac{1}{s - \mathcal{M}_\Delta^2 + iM_\sigma \Gamma_\Delta},
\tag{C1}
$$

where

$$
\begin{aligned}
\mathcal{M}_\Delta^2(s) = \mu^2 + \frac{f_\pi^2(M_\sigma^2 - \mu^2)[f_\pi^2 - (M_\sigma^2 - \mu^2)\bar{R}]}{[f_\pi^2 - (M_\sigma^2 - \mu^2)\bar{R}]^2 + (M_\sigma^2 - \mu^2)^2 I^2}, \\
M_\sigma \Gamma_\Delta(s) = -\frac{f_\pi^2(M_\sigma^2 - \mu^2)^2 I}{[f_\pi^2 - (M_\sigma^2 - \mu^2)\bar{R}]^2 + (M_\sigma^2 - \mu^2)^2 I^2}.
\end{aligned}
\tag{C2}
$$

Comparing this result with Eqs. (21) and (22), we note that $\bar{T}$ and the propagator $\bar{\Delta}$ yield definitions for the resonance mass and width which correspond to different prescriptions for the determination of the renormalization parameter c.

APPENDIX D: EXTENDED σ-MODEL

In order to include another resonance in the linear σ-model, one introduces a second scalar-isoscalar field ξ, which is assumed to be a chiral scalar. The fact that this new field is invariant under both isospin and axial SU(2) × SU(2) transformations allows its physical content to be compatible with structures outside the SU(2) sector such as, for instance, $s\bar{s}$ or glueball states.

Renormalizability is preserved by avoiding couplings with negative dimensions and two new chiral invariant terms are added to the $\mathcal{L}_\sigma$ of Eq. (6), which becomes

$$
\mathcal{L}_{\sigma\xi} = \mathcal{L}_\sigma + \frac{1}{2}(\partial_\mu \xi \partial^\mu \xi - M_\xi^2 \xi^2) + g\xi(\sigma^2 + \boldsymbol{\pi}^2),
\tag{D1}
$$

where M_ξ is the ξ mass and g is a coupling constant. When the σ is reexpressed in terms of the fluctuation f, the new interaction Lagrangian gives rise to a contribution linear in ξ, indicating that this field also has a classical component,

FIG. 14. Counterterm structure for $T_1(s)$.

denoted by e. Writing $\sigma = f_\pi + f$ and $\xi = e + \epsilon$, we find

$$\begin{aligned}
\mathcal{L}_{\sigma\xi} &= [-(m^2/2 - ge)f_\pi^2 - \lambda f_\pi^4/4 + cf_\pi] + [-(m^2 \\
&\quad - 2ge)f_\pi - \lambda f_\pi^3 + c]f + \tfrac{1}{2}[\partial_\mu \boldsymbol{\pi} \cdot \partial^\mu \boldsymbol{\pi} \\
&\quad - (m^2 - 2ge + \lambda f_\pi^2)\boldsymbol{\pi}^2] + \tfrac{1}{2}\partial_\mu f \partial^\mu f - (m^2 \\
&\quad - 2ge + 3\lambda f_\pi^2)f^2] - [\lambda f_\pi f(f^2 + \boldsymbol{\pi}^2) + \lambda \boldsymbol{\pi}^4/4 \\
&\quad + \cdots] + [-M_\xi^2 e + g f_\pi^2]\epsilon + \tfrac{1}{2}(\partial_\mu \epsilon \partial^\mu \epsilon - M_\xi^2 \epsilon^2) \\
&\quad + g\epsilon(f^2 + \boldsymbol{\pi}^2) + 2g f_\pi f \epsilon.
\end{aligned} \quad (D2)$$

The conditions $[-(m^2 - 2ge)f_\pi - \lambda f_\pi^3 + c] = 0$ and $[-M_\xi^2 e + g f_\pi^2] = 0$ for the free parameters allow the elimination of the linear terms in f and ϵ. The $\boldsymbol{\pi}$ and σ masses are

$$\mu^2 = m^2 - 2ge + \lambda f_\pi^2, \qquad M_\sigma^2 = \mu^2 + 2\lambda f_\pi^2. \quad (D3)$$

The last term in Eq. (D2) corresponds to a mass mixing, which is eliminated by introducing new fields α and β, given by

$$\alpha = \cos\theta f + \sin\theta \epsilon, \qquad \beta = -\sin\theta f + \cos\theta \epsilon, \quad (D4)$$

and choosing the angle θ such that $\tan 2\theta = 4g f_\pi/(M_\xi^2 - M_\sigma^2)$. This yields

$$\begin{aligned}
\cos^2\theta M_\alpha^2 + \sin^2\theta M_\beta^2 &= M_\sigma^2, \\
\sin^2\theta M_\alpha^2 + \cos^2\theta M_\beta^2 &= M_\xi^2,
\end{aligned} \quad (D5)$$

and the Lagrangian becomes

$$\begin{aligned}
\mathcal{L}_{\sigma\xi} &= \tfrac{1}{2}[\partial_\mu \boldsymbol{\pi} \cdot \partial^\mu \boldsymbol{\pi} - \mu^2 \boldsymbol{\pi}^2] + \tfrac{1}{2}[\partial_\mu \alpha \partial^\mu \alpha - M_\alpha^2 \alpha^2] \\
&\quad + \tfrac{1}{2}[\partial_\mu \beta \partial^\mu \beta - M_\beta^2 \beta^2] - f_\pi(\lambda_\alpha \alpha + \lambda_\beta \beta)\boldsymbol{\pi}^2 \\
&\quad - \lambda \boldsymbol{\pi}^4/4 + \cdots,
\end{aligned} \quad (D6)$$

where the coupling constants λ_α, λ_β, and λ are completely determined by the masses and mixing angle as

$$\begin{aligned}
\lambda_\alpha &= \cos\theta(M_\alpha^2 - \mu^2)/2f_\pi^2, \\
\lambda_\beta &= -\sin\theta(M_\beta^2 - \mu^2)/2f_\pi^2,
\end{aligned} \quad (D7)$$

$$\lambda = [\cos^2\theta(M_\alpha^2 - \mu^2) + \sin^2\theta(M_\beta^2 - \mu^2)]/2f_\pi^2. \quad (D8)$$

The tree amplitude for $\pi\pi$ scattering is given by the diagrams of Fig. 8 and reads

$$\begin{aligned}
A_t(s, t, u) &= -2\lambda - \frac{4\lambda_\alpha^2 f_\pi^2}{s - M_\alpha^2} - \frac{4\lambda_\beta^2 f_\pi^2}{s - M_\beta^2} \\
&= \frac{s - \mu^2}{f_\pi^2} - \cos^2\theta \frac{(s - \mu^2)^2}{f_\pi^2(s - M_\alpha^2)} \\
&\quad - \sin^2\theta \frac{(s - \mu^2)^2}{f_\pi^2(s - M_\beta^2)}.
\end{aligned} \quad (D9)$$

This result generalizes Eq. (8) and is consistent with the low-energy theorem.

[1] F. E. Close, AIP Conf. Proc. **717**, 919 (2004).
[2] E. M. Aitala *et al.* (E791 Collaboration), Phys. Rev. Lett. **86**, 770 (2001).
[3] E. M. Aitala *et al.* (E791 Collaboration), Phys. Rev. Lett. **89**, 121801 (2002).
[4] H. Muramatsu *et al.* (CLEO Collabotration), Phys. Rev. Lett. **89**, 251802 (2002).
[5] K. Abe *et al.* (Belle Collaboration), hep-ex/0308043.
[6] B. Aubert *et al.* (*BABAR* Collaboration), hep-ex/0408088.
[7] A. Aloisio *et al.* (KLOE Collaboration), Phys. Lett. B **537**, 21 (2002).
[8] J.-Z. Bai *et al.* (BES Collaboration), High Energy Phys. Nucl. Phys. **28**, 215 (2004).
[9] B. Aubert *et al.* (*BABAR* Collaboration), hep-ex/0408032.
[10] N. A. Törnqvist, Z. Phys. C **68**, 647 (1995).
[11] D. V. Bugg, A. V. Sarantsev, and B. S. Zou, Nucl. Phys. **B471**, 59 (1996).
[12] Z. Xiao and H. Zheng, Nucl. Phys. **A695**, 273 (2001).
[13] J. Gasser and H. Leutwyler, Ann. Phys. (N.Y.) **158**, 142 (1984).
[14] S. Weinberg, Phys. Rev. Lett. **17**, 616 (1966).
[15] S. Weinberg, Phys. Rev. **166**, 1568 (1968).
[16] C. M. Maekawa and M. R. Robilotta, Phys. Rev. C **57**, 2839 (1998).
[17] J. L. Basdevant and B. W. Lee, Phys. Rev. D **2**, 1680 (1970).
[18] J. Sá Borges, Nucl. Phys. **B51**, 189 (1973).
[19] B. W. Lee, Nucl. Phys. **B9**, 649 (1969); B. W. Lee and J. L. Gervais, Nucl. Phys. **B12**, 627 (1969); B. W. Lee, *Chiral Dynamics* (Gordon and Breach, New York, 1972).
[20] M. E. Peskin and D. V. Schroeder, *An Introduction to Quantum Field Theory* (Addison-Wesley, Reading, MA, 1995), Chap. 11.
[21] G. Colangelo, J. Gasser, and H. Leutwyler, Nucl. Phys. **B603**, 125 (2001).
[22] N. N. Achasov and G. N. Shestakov, Phys. Rev. D **49**, 5779 (1994).
[23] D. Black, A. H. Fariborz, S. Moussa, S. Nasri, and J. Schechter, Phys. Rev. D **64**, 014031 (2001).
[24] S. Gasiorowicz and D. A. Geffen, Rev. Mod. Phys. **41**, 531 (1969).
[25] J. A. Oller and E. Oset, Nucl. Phys. **A620**, 438 (1997); Nucl. Phys. **A652**, 407(E) (1999); J. A. Oller, E. Oset, and J. R. Peláez, Phys. Rev. D **59**, 074001 (1999); J. A. Oller and E. Oset, Phys. Rev. D **60**, 074023 (1999).
[26] M. Svec, Phys. Rev. D **64**, 096003 (2001).
[27] Chiral Dynamics—Theory and Experiment III: Proceedings from the Institute for Nuclear Theory 11, edited by A. M. Bernstein, J. L. Goity, and Ulf-G. Meissner (World Scientific, Singapore, 2001).